

Evolution of optical properties and molecular structure of PCBM films under proton irradiation

Guo-Dong Xiong(熊国栋), Hui-Ping Zhu(朱慧平), Lei Wang(王磊), Bo Li(李博), Fa-Zhan Zhao(赵发展), and Zheng-Sheng Han(韩郑生)

Citation: Chin. Phys. B, 2022, 31 (**5**): 057102. DOI: 10.1088/1674-1056/ac322b
Journal homepage: http://cpb.iphy.ac.cn; http://iopscience.iop.org/cpb

What follows is a list of articles you may be interested in

Ab initio study of structural, electronic, thermo-elastic and optical properties of Pt_3Zr intermetallic compound

Wahiba Metiri, Khaled Cheikh
Chin. Phys. B, 2020, 29 (**4**): 047101. DOI: 10.1088/1674-1056/ab7223

First principles investigation of protactinium-based oxide-perovskites for flexible opto—electronic devices

Nazia Erum, Muhammad Azhar Iqbal
Chin. Phys. B, 2017, 26 (**4**): 047102. DOI: 10.1088/1674-1056/26/4/047102

The nonlinear optical properties of a magneto-exciton in a strained $Ga_{0.2}In_{0.8}As$/GaAs quantum dot

N. R. Senthil Kumar, A. John Peter, Chang Kyoo Yoo
Chin. Phys. B, 2013, 22 (**10**): 107106. DOI: 10.1088/1674-1056/22/10/107106

Electronic structure of PCBM

Sheng Chun-Qi, Wang Peng, Shen Ying, Li Yan-Jun, Zhang Wen-Hua, Xu Fa-Qiang, Zhu Jun-Fa, Lai Guo-Qiao, Li Hong-Nian
Chin. Phys. B, 2012, 21 (**1**): 017102. DOI: 10.1088/1674-1056/21/1/017102

Density-functional theory investigation of energy gaps and optical properties of $Hg_{1-x}Cd_xTe$ and $In_{1-x}Ga_xAs$

Guo San-Dong, Liu Bang-Gui
Chin. Phys. B, 2012, 21 (**1**): 017101. DOI: 10.1088/1674-1056/21/1/017101

Evolution of optical properties and molecular structure of PCBM films under proton irradiation

Guo-Dong Xiong(熊国栋)[1,2], Hui-Ping Zhu(朱慧平)[1,†], Lei Wang(王磊)[1], Bo Li(李博)[1,‡], Fa-Zhan Zhao(赵发展)[1], and Zheng-Sheng Han(韩郑生)[1,2,§]

[1] *Key Laboratory of Science and Technology on Silicon Devices, Institute of Microelectronics, Chinese Academy of Sciences, Beijing* 100029, *China*

[2] *University of the Chinese Academy of Sciences, Beijing* 100049, *China*

(Received 7 September 2021; revised manuscript received 12 October 2021; accepted manuscript online 22 October 2021)

Low-energy proton irradiation effects on the optical properties and the molecular structure of phenyl-C_{61}-butyric acid methyl ester (PCBM) are studied in this work. The PCBM films are irradiated by 100-keV proton beams with fluences of 5×10^{12} p/cm^2, 5×10^{13} p/cm^2, and 5×10^{14} p/cm^2, respectively. The photoluminescence (PL) peaks of the post-irradiated PCBM films show a progressive decrease in the peak intensity as the proton fluences increase, which can be attributed to the deep defect levels induced by proton irradiation. Additionally, a slight blue-shift in the PL spectrum is also observed at a proton fluence of 5×10^{14} p/cm^2. The underlying mechanism can be traced back to the lift of the lowest unoccupied molecular orbital (LUMO) level, which is caused by the attachment of methoxy radicals on ortho position of the phenyl ring in the post-irradiated PCBM structure. This work is of significance in understanding the radiation hardness and the damage mechanism of the PCBM film in radiation environments, which is essential before it is put into practical application in space.

Keywords: PCBM, proton irradiation effects, optical property, molecular structure

PACS: 71.20.Tx, 73.61.Wp, 78.30.Na, 78.66.Tr **DOI:** 10.1088/1674-1056/ac322b

1. Introduction

Since excellent electron-accepting capability of fullerene and their derivatives,[1] phenyl-C_{61}-butyric acid methyl ester (PCBM, $C_{72}H_{14}O_2$) has been widely applied to the hybrid perovskite optoelectronic devices, such as solar cells,[2,3] and photo-diodes,[4] and photodetector.[5] On the one hand, it is employed to transfer the photo-generated carries coming from the perovskite active layer and acts as an electron transport layer.[6] On the other hand, it can also eliminate the deep trap centers by passivating the dangling bonds on the perovskite grain boundary surfaces.[7–10] The excessive halide anions (such as I) located on the grain boundaries of hybrid perovskites become electronic traps. When the PCBM is homogeneously distributed on the active layer surface, the bonding between PCBM and defective halides can not only suppress the formation of deep traps, but also make them much shallower. Therefore, the PCBM plays a significant role in the hybrid perovskite optoelectronic devices.[11–13]

Recently, the certified power conversion efficiency (PCE) of solar cells fabricated with hybrid perovskite materials has achieved 25.5%, which is comparable to the PCE of traditional silicon-based solar cells.[2] Moreover, the hybrid perovskite materials even exhibit much higher radiation hardness than Si, GaAs, and GaN materials.[14,15] Therefore, hybrid perovskite solar cells as well as related other photoelectric devices have great potential applications in space.[16] However, the organic functional materials in the photoelectric devices, such as the PCBM electron transfer layer, are extremely sensitive to the irradiation existing in space.[6] The deterioration of the organic functional layers under radiation environments results in the severe performance degradation of the photoelectric devices. As a result, the researches on the irradiation effects of the PCBM films are urgently required for the future applications in space to ensure the stable operation of the photoelectric devices.[17]

To date, most of studies on the irradiation effects of the PCBM films have focused mainly on electron[18,19] and heavy ion irradiation.[20] For instance, Yoo *et al.* reported that the bandgaps of the PCBM films can be controlled by electron irradiation and an increasement of the bandgap is observed after having been irradiated.[19] Additionally, previous research has also found a decrease in the bandgap of the PCBM film after having been irradiated by 55-MeV Si^{4+} ions.[20] However, few studies have attempted to explore the influence of proton irradiation on the PCBM films and reveal their damage mechanism. As is well known, the proton irradiation is unavoidable for the photoelectric devices working in space environments, protons being the main energetic particles in space.[17] In our previous work, the proton irradiation effects of the PCBM

†Corresponding author. E-mail: zhuhuiping@ime.ac.cn
‡Corresponding author. E-mail: libo3@ime.ac.cn
§Corresponding author. E-mail: zshan@ime.ac.cn

© 2022 Chinese Physical Society and IOP Publishing Ltd

functional layer in hybrid perovskite photodetectors were simply studied.[6] Nevertheless, little is known about the damage mechanism of the PCBM films caused by the low-energy proton irradiation and it is not clear about the evolution of the bandgap after irradiation.

In this work, we investigate the proton irradiation effects of PCBM and reveal the relationship between the molecular structure and the band structure of the PCBM films irradiated by protons with different fluences. A significant decrease of luminescence intensity is observed in post-irradiated PCBM, indicated by PL spectra. Then, the molecular structures of PCBM films and variations of functional groups in different stages are characterized by Raman spectra, x-ray photoelectron spectroscopy (XPS), and Fourier transform infrared (FTIR) spectra. Finally, the evolution process of the defects under different irradiation fluences is summarized, which is in accordance with the variation of the molecular structures. These findings are expected to be conducive to the applications of hybrid perovskite devices in space in the future.

2. Experiment

In this study, the PCBM films were prepared by spin-coating technology on the indium tin oxide (ITO) glass substrates at a spin rate of 1500 rpm for 60 s, which were previously cleaned by detergent, deionized water and ethanol in an ultra-sonic bath (30 min for each step). Film thickness was typically 50 nm.

The proton irradiation experiments were carried out in the proton accelerator in Harbin Institute of Technology. The energy of proton particles was 100 keV. The samples were irradiated in a vacuum accelerator chamber under 10^{-4} Pa at room temperature. They were irradiated by proton beam with fluences of 5×10^{12} p/cm^2, 5×10^{13} p/cm^2, and 5×10^{14} p/cm^2, respectively. A group of reference PCBM films kept in N_2 ambient during irradiation experiments were employed as the pre-irradiated samples in our experiments for comparison with the post-irradiated ones so that we can exclude the variation of the samples caused by the intrinsic decay of the film itself.

Raman and PL spectra were measured with a laser wavelength of 532 nm. Fourier transform infrared (FTIR) spectroscopy measurements were used to characterize the change of functional groups in PCBM molecules with different proton irradiation fluences. The x-ray photoelectron spectroscopy (XPS) measurements were carried out to detect chemical bonds of the PCBM films. All irradiation experiments and measurements were performed at room temperature in ambient conditions. Stopping and ranges of ions in matter (SRIM) software is used for evaluating the displacement damage to the PCBM films induced by proton irradiation.[21]

3. Results and discussion

Figure 1 presents the PL spectra of the pre- and post-irradiated PCBM films with proton fluences of 5×10^{12} p/cm^2, 5×10^{13} p/cm^2, and 5×10^{14} p/cm^2. The graph displays that the pre-irradiated PCBM film has an emission peak located at $\sim$ 736 nm, which is attributed to the emission from the intramolecular transition in a PCBM molecule.[22,23] The intensities of PL spectra of the irradiated PCBM films drop gradually with the increase of proton fluence, and the emission peak almost quenches at a high proton fluence of 5×10^{14} p/cm^2, demonstrating that the PCBM molecules have been severely destroyed[19,22] and the intramolecular photon emission is suppressed. The decline of PL intensity originates from the electron trap centers located in the bandgap of the PCBM. In our previous study,[6] the band structure of the PCBM with the defects of methoxy radical vacancy (V_{OCH3}) was investigated by first-principles calculations. The results reveal that deep defect levels in the first energy gap and the second energy gap are introduced by V_{OCH3} and act as electron trap centers. Therefore, the deep defect levels caused by V_{OCH3} can trap electrons in the PCBM layer and degrades the optical properties.

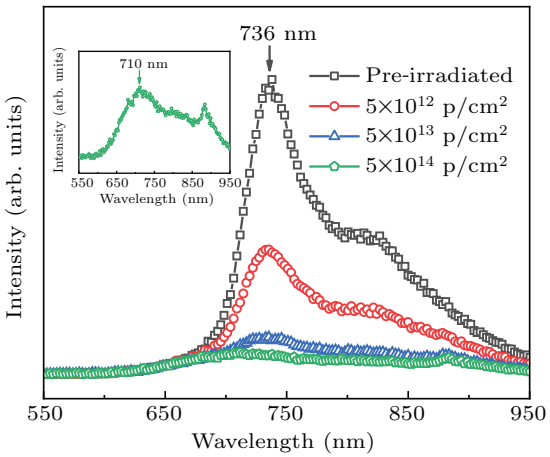


Fig. 1. PL spectra of the PCBM film before and after proton irradiations, with inset showing corresponding PL spectrum of PCBM film with proton fluence of 5×10^{14} p/cm^2.

Additionally, we find that the damage at low irradiation fluences, such as 5×10^{12} p/cm^2 and 5×10^{13} p/cm^2, has a negligible effect on the emission peak position located at $\sim$ 736 nm. However, a slight blue-shift of the PL peak from 736 nm (1.68 eV) to 710 nm (1.75 eV) is observed at the fluence of 5×10^{14} p/cm^2 as illustrated in Fig. 1. This suggests that the bandgap (E_g) of the PCBM film can be engineered by the proton irradiation. The detailed analysis will be discussed as follows.

The SRIM simulation was used to analyze the defect types induced by proton irradiation in the PCBM films.[21] The proton beam energy and the density of PCBM are set to be 100 keV and 2.5 g/cm^2, respectively. The breakage of covalence bonds upon irradiation in organic materials is well

known.[24] Therefore, the collisions between the energic protons and target atoms will give rise to the dissociation of the covalence bonds in the PCBM films into C–C, C–H, and C–O bonds. As shown in Fig. 2, there are three types of vacancy defects, namely, carbon vacancy (V_C), hydrogen vacancy (V_H), and oxygen vacancy (V_O), in the irradiated PCBM film. And V_C is identified as the primary defects in PCBM, suggesting that the poor crystallinity of PCBM after proton irradiation is assigned mainly to the formation of V_C. Besides, the concentrations of all the vacancy defects show a gradually increasing trend with the increase of proton incident depth, implying that more serious damage is introduced towards the bottom part of each PCBM film.

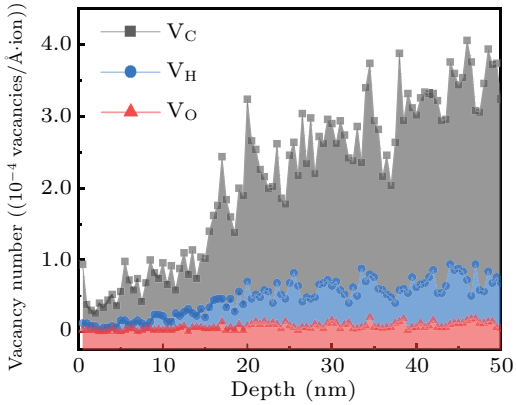


Fig. 2. Number of vacancies *versus* depth for carbon vacancy (V_C), hydrogen vacancy (V_H), and oxygen vacancy (V_O), in the PCBM films induced by proton irradiation.

The main source of carbon element is from the C_{60} cage in the PCBM molecule. For the more detailed explanation of the displacement damage to the PCBM film, pre- and post-irradiated PCBM films are analyzed by Raman spectra, as displayed in Fig. 3. For the pre-irradiated PCBM films, three typical Raman vibration modes, $H_g(7)$, $A_g(2)$, and $H_g(8)$, are clearly seen at 1425 cm^{-1}, 1460 cm^{-1}, and 1566 cm^{-1}, respectively. The peak positions are consistent with previously reported results.[19,20,25] Among these modes, the most intense Raman mode located at 1460 cm^{-1} corresponds to the "pentagonal pinch mode", which originates from the vibration of the C_{60} cage in PCBM.[26] As shown in Fig. 3, the full width at half maximum (FWHM) increases progressively in the $A_g(2)$ mode. The FWHM of the pre-irradiated PCBM film is about 8.05 cm^{-1} and then increases to 9.43 cm^{-1} at an irradiation fluence of 5×10^{13} p/cm^2. It disappears almost entirely when the irradiation fluence rises to 5×10^{14} p/cm^2, implying that the C_{60} cage has been seriously destroyed, and part of C_{60} cage is transformed into amorphous carbon structure.[19,20,23,26]

In summary, SRIM simulation and Raman spectra suggest that the significant degradation of the optical property can be attributed to the displacement damage to the PCBM films. These defects give rise to the introduction of deep defect levels into the bandgap of the PCBM, which act as non-radiative recombination centers, thereby reducing the PL intensity.[6]

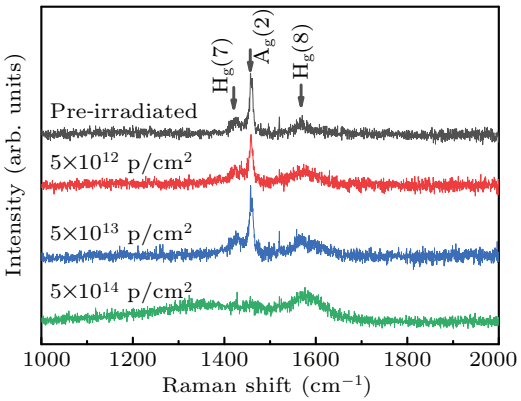


Fig. 3. Raman spectra of PCBM films before and after proton irradiations with different fluences.

Beside the significant degradation of optical property, the most striking finding is that the E_g of PCBM increases from 1.68 eV to 1.75 eV at a proton fluence of 5×10^{14} p/cm^2 as observed in Fig. 1. This increase of E_g may be explained by the change of the PCBM molecule structure after having been irradiated by protons . To reveal the underlying mechanism of the modification, XPS and FTIR spectroscopy are adopted. Figures 4(a) and 4(b) show the O 1s and C 1s core level spectra of the PCBM films, respectively. For the pre-irradiated PCBM film in Fig. 4(a), two peaks located at ∼ 533.3 eV and ∼ 531.8 eV arise from the butyric acid methyl ester side chain of PCBM and correspond to the C–O bond and C=O bond, respectively.[27,28] In this case, those two peaks have almost equivalent intensity. However, the peak intensity of the C–O bond decreases sharply with the fluence increasing up to 5×10^{12} p/cm^2. Unlike the C–O bond, the C=O bond has the peak intensity that is almost unchanged. These results suggest that the C–O bond is easier to break under proton irradiation, forming methoxy radicals.[14] It is worth mentioning that a new peak located at about ∼ 533.5 eV occurs when the proton fluence increases to 5×10^{13} p/cm^2 and 5×10^{14} p/cm^2, separately. Previous research has reported that the O 1s characteristic peak at binding energy ∼ 533.5 eV originates from the C–O–C bond of ether.[27]

Figure 4(b) shows that the XPS spectra of all the samples can be divided into five peaks according to the peak decomposition data.[10,28,29] They are assigned to shake-up π–π^* satellite, carbonyl C from the methyl ester, methoxy C of the methyl ester group, saturated C atoms of the butyl chain, and conjugated C atoms of the C_{60} fullerene and phenyl group, respectively. The C–O and C=O bonds, which are located at ∼ 286.2 eV and ∼ 288.8 eV, separately, also originate from the butyric acid methyl ester side chain, which is the same as the results in Fig. 4(a). The C–C bond and C=C bond located at ∼ 285.3 eV and ∼ 284.8 eV are assigned to the C atoms of the butyl chain and the fullerene, respectively. The peak located at ∼ 291.2 eV corresponding to the shake-up π–π^* satellite is associated with the transition from highest occupied molecular orbital (HOMO) level to lowest unoccupied molecular orbital

(LUMO) level.[22] On the one hand, the relative intensity of the C=O bond has no significant change with proton irradiation fluence increasing from 5×10^{12} p/cm^2 to 5×10^{14} p/cm^2 as shown in Fig. 4(b), implying that the C=O bond has better stability than the C–O bond due to its stronger bonding energy. The results are consistent with the variation trend of C=O bonds in Fig. 4(a). On the other hand, the intensity of C–O bond decreases progressively with fluence lowering, which is similar to the variation trend of C–O bond in O 1s core level in Fig. 4(a). However, it is worth pointing out that a remarkable increase of C–O bond peak is observed at proton fluence of 5×10^{14} p/cm^2. The C–O peak in XPS spectra originates from the functional groups, which contain C–O bonds, such as C–O bond and C–O–C bond. In other words, the signal of C–O peak in XPS spectrum is the accumulation of signals of all functional groups containing the C–O bonds. The formation of the C–O–C bonds on the phenyl ring can increase the intensity of the C–O peaks as shown in Fig. 4(b).[28] Therefore, the increase in C–O bonds can be attributed to the formation of C–O–C bonds. These results are consistent with the data obtained in O 1s core level spectra and further confirm the relation between C–O peaks and C–O–C bonds in XPS spectra. In other words, C–O–C bonds can be formed in the PCBM films irradiated by protons with fluences of 5×10^{13} p/cm^2 and 5×10^{14} p/cm^2.

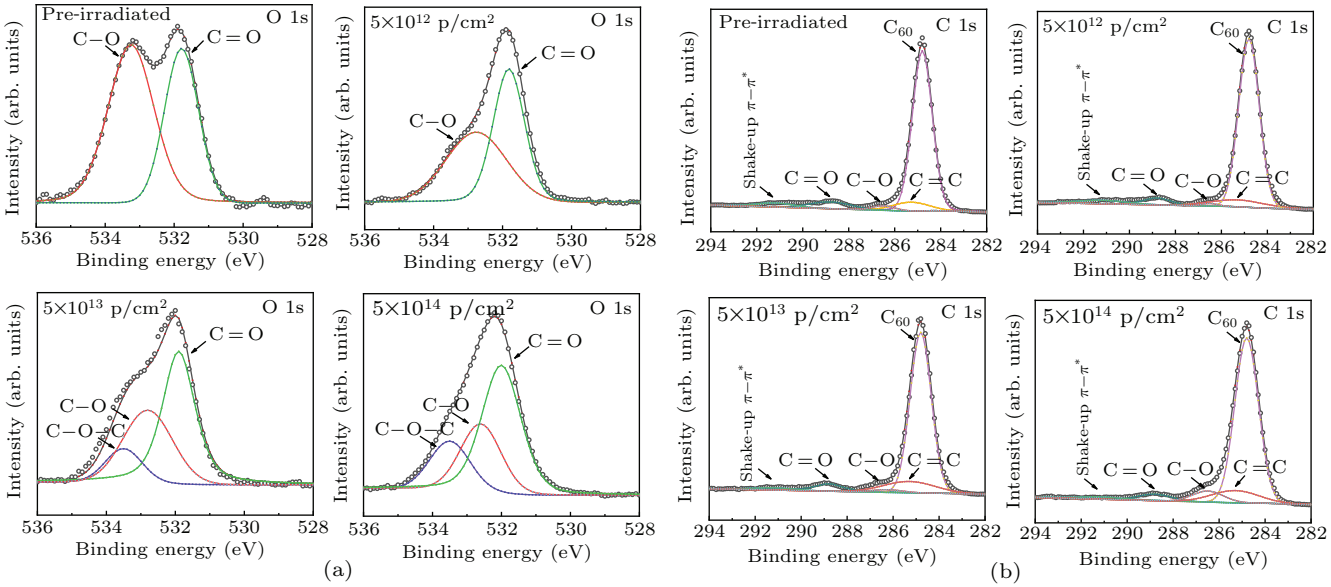


Fig. 4. XPS spectra of PCBM films before and after being irradiated by neutrons, showing (a) O 1s core level, (b) C 1s core level, with black circles representing raw data of XPS spectra.

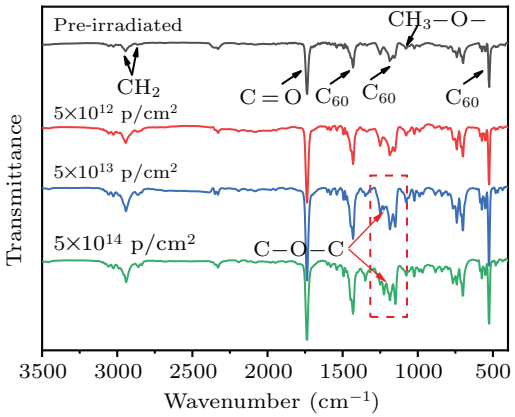


Fig. 5. FTIR spectra of the PCBM films before and after having been irradiated by protons with different fluences, with red arrows pointing to the positions of C–O–C vibration modes.

To further confirm the molecule structure modification, the FTIR spectra of PCBM films irradiated by protons with different fluences are recorded. Figure 5 gives the FTIR spectra of PCBM films in a wavenumber range from 3500 cm^{-1} to 400 cm^{-1}. The adsorption peaks at 2940 cm^{-1} and 2855 cm^{-1} are attributed to asymmetric and symmetric C–H stretching modes in CH_2 groups,[30] respectively. The peak located at 1740 cm^{-1} corresponds to C=O group of butyric acid methyl ester side chain.[31] And the peak at 1080 cm^{-1} is the C–O characteristic peak of methoxy group.[32] The other peaks at 1189 cm^{-1}, 573 cm^{-1}, and 525 cm^{-1} are associated with the fullerene.[30] It can be observed that the main types of the functional groups in the PCBM films are almost unchanged at a proton fluence of 5×10^{12} p/cm^2. However, a new peak occurs at 1225 cm^{-1} when proton fluence reaches 5×10^{13} p/cm^2 and 5×10^{14} p/cm^2, separately (the peak position is marked with red arrow), and its intensity is higher at 5×10^{14} p/cm^2. This new infrared active mode is caused by the asymmetric C–O–C stretching mode of aryl ether.[33] In summary, the appearing of the peak around 1225 cm^{-1} in the FTIR spectrum further supports the idea that C–O–C bonds have formed in PCBM films under the high-influence irradiation.

To understand the evolution of molecular structure and defects of PCBM under the irradiation of protons with different fluences, figure 6 provides the schematic illustration in

different stages in detail. Figure 6(a) shows the ideal molecular structure of the PCBM. As a fullerene derivative, its main structure is C_{60} cage, the other two functional groups are phenyl ring and butyric acid methyl ester side chain. After the irradiation by low-fluence protons, the C–O bonds in the butyric acid methyl ester side chain are decomposed gradually due to lower bond energy of C–O bonds, producing methoxy radicals, as illustrated in Fig. 6(b). At this moment, the presence of V_{OCH3} leads the PL intensity to decrease due to the deep trap centers located in the bandgap of PCBM. In addition, the C–H bonds in the phenyl ring are also broken at the same time, resulting in the formation of the phenyl radicals. With the increasing of irradiation fluences, the C_{60} will be destroyed gradually and even transformed into amorphous carbon structure after having been irradiated by higher-fluence protons, resulting in further decrease in PL intensity. At this moment more energy can be deposited and transfer to the PCBM films by electron–phonon coupling.[20,34,35] Consequently, the temperature of the regions irradiated by high-fluence protons increases immediately due to the formation of thermal spike in nanoscale region.[36] The remarkable increase of the temperature in local region is beneficial to the polymerization reactions between methoxy radicals and defective PCBM film as displayed in Fig. 6(c).

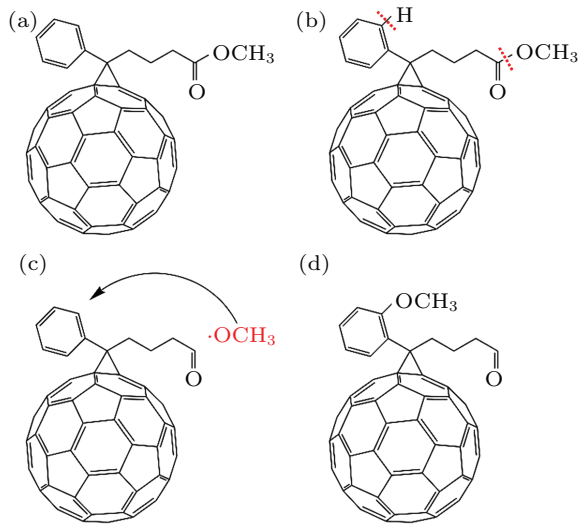


Fig. 6. Schematic illustration of modification in molecular structure of PCBM by proton irradiation showing (a) an ideal PCBM molecular structure, (b) formation of methoxy radical and phenyl ring radical at low proton irradiation fluence, two kinds of active radicals originating from the breakage of C–O bonds and C–H bonds, respectively. (c) Methoxy radical combining with phenyl ring (the positions 1, 2, and 3 correspond to the ortho, meta, and para positions of phenyl ring, respectively), and (d) formation of C–O–C bonds between methoxy radical and phenyl ring under high-fluence proton irradiation.

The position evolution of the methoxy radical on the phenyl ring irradiated by protons with a fluence of 5×10^{14} p/cm^2 will be discussed briefly below. In this stage, more methoxy radicals and phenyl radicals appear in irradiated PCBM and can act as the reactants for polymerization reactions. Previous study found that the increase of PCBM bandgap before and after irradiations are caused mainly by the change of LUMO levels, and HOMO levels are almost unchanged.[19] Therefore, the phenomenon of blue-shift in Fig. 1 is likely to be due to the lift of the LUMO level. Morvillo *et al*. performed the energy band calculations of PCBM with different substituent groups, and reported that the LUMO level of PCBM is increased by 0.08 eV, 0.04 eV, and 0.02 eV after the methoxy group has attached to the ortho 1, meta 2, and para 3 positions of phenyl ring, respectively.[37] The increase of bandgap at 5×10^{14} p/cm^2 is about 0.07 eV, which is similar to the change of LUMO level at ortho position (position 1 in Fig. 6(c)). The results indicate that the methoxy radicals are most likely located at ortho position of phenyl ring under high-fluence protons. In the end, the methoxy radicals form C–O–C covalent bonds with irradiated PCBM molecules as displayed in Fig. 6(d).

4. Conclusions

In this paper, the variations of the optical properties of the PCBM films under the irradiation of protons with different fluences are investigated in detail. The results show that the PL intensity decreases sharply after the PCBM film has been irradiated by the protons with fluences from 5×10^{12} p/cm^2 p/cm^2 to 5×10^{14} p/cm^2. Moreover, a slight blue-shift of PL spectrum is observed when the irradiation fluence reaches 5×10^{14} p/cm^2, implying the enlargement of the bandgap. The polymerization reaction between methoxy radicals and phenyl ring in the irradiated PCBM film results in the blue-shift of the PL spectrum. The combination of the experimental results with the simulation results reveals the detailed decomposition process and the origin of blue-shift of PL spectrum of PCBM after being irradiated by protons, which is quite important for the long-term stability of hybrid perovskite devices operating in the space environments.

Acknowledgements

Project supported by the Youth Innovation Promotion Association, Chinese Academy of Sciences, the National Natural Science Foundation of China (Grant No. 61874135), and the Foundation of Frontier Science of the Chinese Academy of Sciences (Grant No. ZDBS-LY-JSC015).

References

[1] Mihailetchi V D, van Duren J K J, Blom P W M, Hummelen J C, Janssen R A J, Kroon J M, Rispens M T, Verhees W J H and Wienk M M 2003 *Adv. Funct. Mater.* **13** 43
[2] Tu Y G, Wu J, Xu G N, Yang X Y, Cai R, Gong Q H, Zhu R and Huang W 2021 *Adv. Mater.* **33** 2006545
[3] Yang J, Bao Q, Shen L and Ding L 2020 *Nano Energy* **76** 105019
[4] Dou L, Yang Y M, You J, Hong Z, Chang W H, Li G and Yang Y 2014 *Nat. Commun.* **5** 5404

[5] Hao D, Zou J and Huang J 2020 *InfoMat.* **2** 139
[6] Xiong G, Qin Z, Li B, Wang L, Zhang X, Zheng Z, Zhu H, Zhao S, Gao J, Li B, Yang J, Li X, Luo J, Han Z, Liu X and Zhao F 2021 *J. Mater. Chem. C* **9** 2095
[7] Yuan Y and Huang J 2016 *Acc. Chem. Res.* **49** 286
[8] Shao Y H, Xiao Z G, Bi C, Yuan Y B and Huang J S 2014 *Nat. Commun.* **5** 5784
[9] Xu J, Buin A, Ip A H, Li W, Voznyy O, Comin R, Yuan M, Jeon S, Ning Z, McDowell J J, Kanjanaboos P, Sun J P, Lan X, Quan L N, Kim D H, Hill I G, Maksymovych P and Sargent E H 2015 *Nat. Commun.* **6** 7081
[10] Zhong Y, Hufnagel M, Thelakkat M, Li C and Huettner S 2020 *Adv. Funct. Mater.* **30** 1908920
[11] Liu Y T, Jia R X, Wang Y C, Hu Z Y, Zhang Y M, Pang T Q, Zhu Y J and Luan S Z 2017 *ACS Appl. Mater. Interfaces* **9** 15638
[12] Kwon K C, Hong K, Van Le Q, Lee S Y, Choi J, Kim K B, Kim S Y and Jang H W 2016 *Adv. Funct. Mater.* **26** 4213
[13] Ran C, Xu J, Gao W, Huang C and Dou S 2018 *Chem. Soc. Rev.* **47** 4581
[14] Lang F, Nickel N H, Bundesmann J, Seidel S, Denker A, Albrecht S, Brus V V, Rappich J, Rech B, Landi G and Neitzert H C 2016 *Adv. Mater.* **28** 8726
[15] Lang F, Jost M, Bundesmann J, Denker A, Albrecht S, Landi G, Neitzert H C, Rappich J and Nickel N H 2019 *Energy Environ. Sci.* **12** 1634
[16] Xiao W, Yang J, Xiong S, Li D, Li Y, Tang J, Duan C and Bao Q 2019 *Sol. RRL.* 1900394
[17] Schwank J R, Shaneyfelt M R and Dodd P E 2013 *IEEE Trans. Nucl. Sci.* **60** 2074
[18] Yoo S H, Kum J M, Ali G, Heo S H and Cho S O 2012 *Nanoscale Res. Lett.* **142** 1
[19] Yoo S H, Kum J M and Cho S O 2011 *Nanoscale Res. Lett.* **6** 545
[20] Sharma T, Singhal R, Vishnoi R, Lakshmi G B V S and Biswas S K 2017 *Nucl. Instrum. Method B* **396** 5
[21] Ziegler J F, Ziegler M D and Biersack J P 2010 *Nucl. Instrum. Method B* **268** 1818
[22] Cook S, Ohkita H, Kim Y, Benson-Smith J J, Bradley D D C and Durrant J R 2007 *Chem. Phys. Lett.* **445** 276
[23] Wang X, Egelhaaf H J, Mack H G, Azimi H, Brabec C J, Meixner A J and Zhang D 2014 *Adv. Energy Mater.* **4** 1400497
[24] Bebensee F, Zhu J F, Baricuatro J H, Farmer J A, Bai Y, Steinruck H P, Campbell C T and Gottfried J M 2010 *Langmuir* **26** 9632
[25] Kuzmany H, Matus M, Burger B and Winter J 1994 *Adv. Mater.* **6** 731
[26] Kumar S, Kumar M, Rathi S, Yadav A, Upadhyaya A, Gupta S K and Singh A 2018 *2nd International Conference on Condensed Matter and Applied Physics,* November 24–25, 2017, Bikaner, India, p. 100074
[27] Lopez G P, Castner D G and Ratner B D 1991 *Surf. Interface Anal.* **17** 267
[28] Lownsbury J M, Sharp J C, Mann E J and Campbell C T 2015 *J. Phys. Chem. C* **119** 18444
[29] Richter M H, Friedrich D and Schmeißer D 2012 *Bionanosci.* **2** 59
[30] Silva E A, Gregori A, Fernandes J D, Njel C, Dedryvere R, Constantino C J L, Hiorns R C, Lartigau-Dagron C and Olivati C A 2020 *Nanotechnol.* **31** 315712
[31] Sharma T, Singhal R, Vishnoi R, Sharma P, Patra A, Chand S, Lakshmi G and Biswas S K 2016 *Nucl. Instrum. Method B* **379** 176
[32] Wu J H, Yue G T, Xiao Y M, Ye H F, Lin J M and Huang M L 2010 *Electrochim. Acta* **55** 5798
[33] Siengchum T, Isenberg M and Chuang S S C 2013 *Fuel.* **105** 559
[34] Jung S H, Jeong I Y, Han W S, Lee S S and Jung J H 2009 *J. Nanosci. Nanotechnol.* **9** 2777
[35] Ju D, Sun C, Wang H, Wang X, Wu Y, Dong Z and Qiu X 2020 *RSC Adv.* **10** 39572
[36] De Cicco H, Saint-Martin G, Alurralde M and Bernaola O A 1999 *Radiat. Meas.* **31** 77
[37] Morvillo P and Bobeico E 2008 *Sol. Energy Mater. Sol. Cells* **92** 1192